

Geophysical Research Letters

Supporting Information for

Upper mantle hydration indicated by decreased shear velocity near the Southern Mariana Trench from Rayleigh wave tomography

Gaohua Zhu¹, Douglas A. Wiens², Hongfeng Yang¹, Jian Lin^{3,4,5}, Min Xu^{3,6}, and Qingyu You⁷

¹Earth System Science Programme, Faculty of Science, the Chinese University of Hong Kong, Shatin, Hong Kong, China

²Department of Earth and Planetary Sciences, Washington University in St Louis, St Louis, MO 63130, USA

³Key Laboratory of Ocean and Marginal Sea Geology, South China Sea Institute of Oceanology, Innovation Academy of South China Sea Ecology and Environmental Engineering, Chinese Academy of Sciences, Guangzhou 511458, China

⁴Department of Ocean Science and Engineering, Southern University of Science and Technology, Shenzhen 518055, China

⁵Department of Geology and Geophysics, Woods Hole Oceanographic Institution, Woods Hole, MA 02543, USA

⁶Southern Marine Science and Engineering Guangdong Laboratory (Guangzhou), 511458, China

⁷Key Laboratory of Petroleum Resources Research, Institute of Geology and Geophysics, Chinese Academy of Sciences, Beijing 100029, China

Contents of this file

Fig. S1 The stacked vertical component ambient noise cross-correlations

Fig. S2 An example of the frequency-time analysis (FTAN) diagram used to make group and phase velocity measurements.

Fig. S3 Maps of the azimuthally averaged group and phase velocities.

Fig. S4 Earthquakes (red dots) used in this study.

Fig. S5 Phase-velocity sensitivity kernels at example periods.

Fig. S6 Robustness test of the low-velocity zone.

Introduction

This file contains 6 supporting figures mostly for the methods section in the main text of the manuscript.

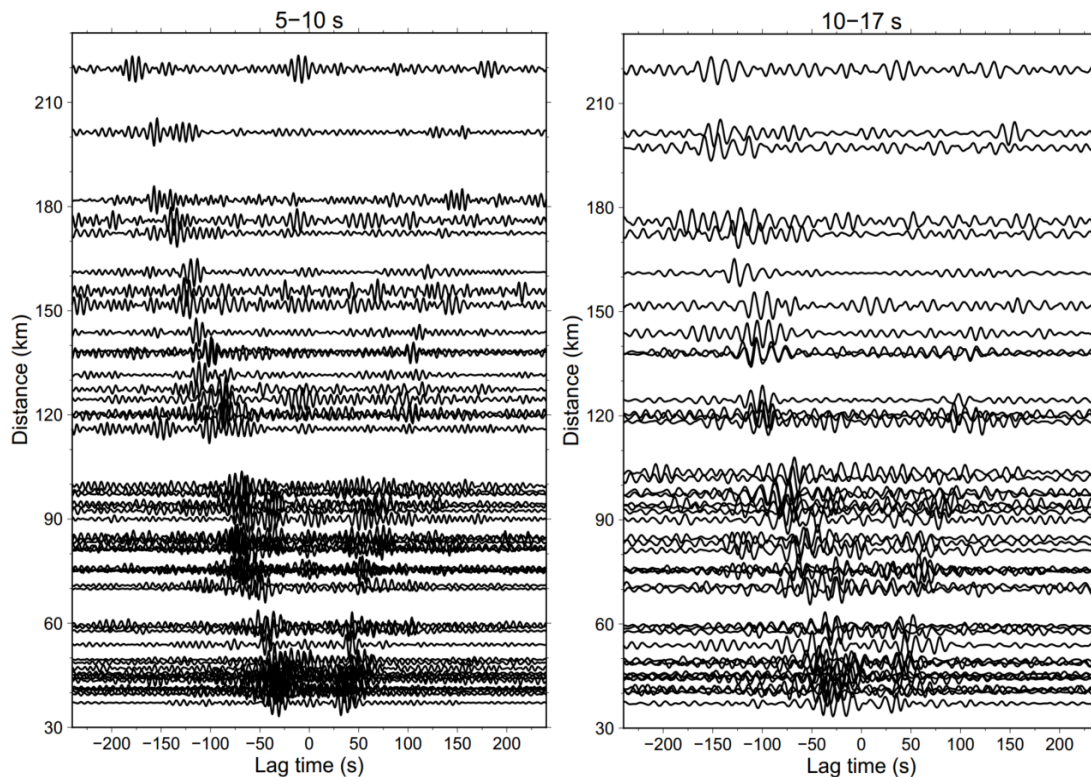


Fig. S1 The stacked vertical component ambient noise cross-correlations between OBS pairs in frequency bands of 5-10 s and 10-17 s. The traces with low signal to noise ratio have been removed.

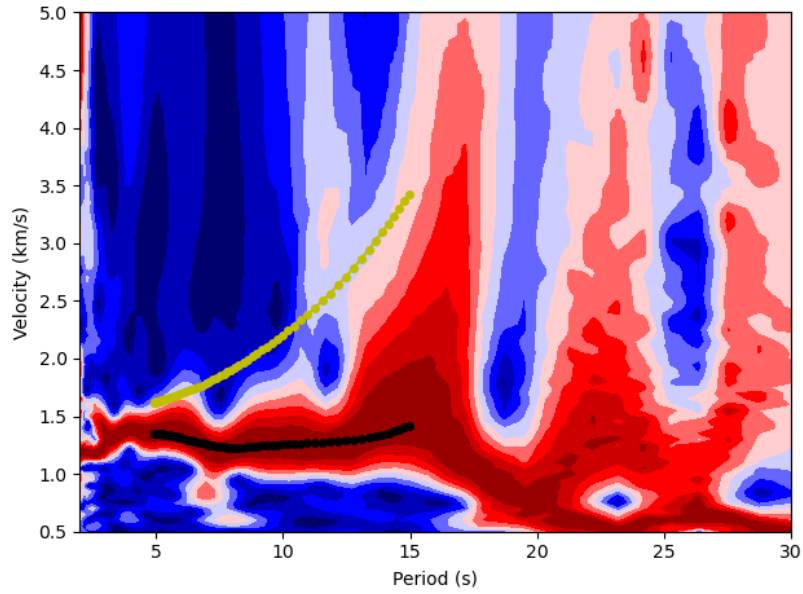


Fig. S2 An example of the frequency-time analysis (FTAN) diagram used to make group and phase velocity measurements. The black and yellow dots represent measured group velocities and estimated phase velocities, respectively. The OBS pairs are PA02 and PG04 with a distance of 92.3 km.

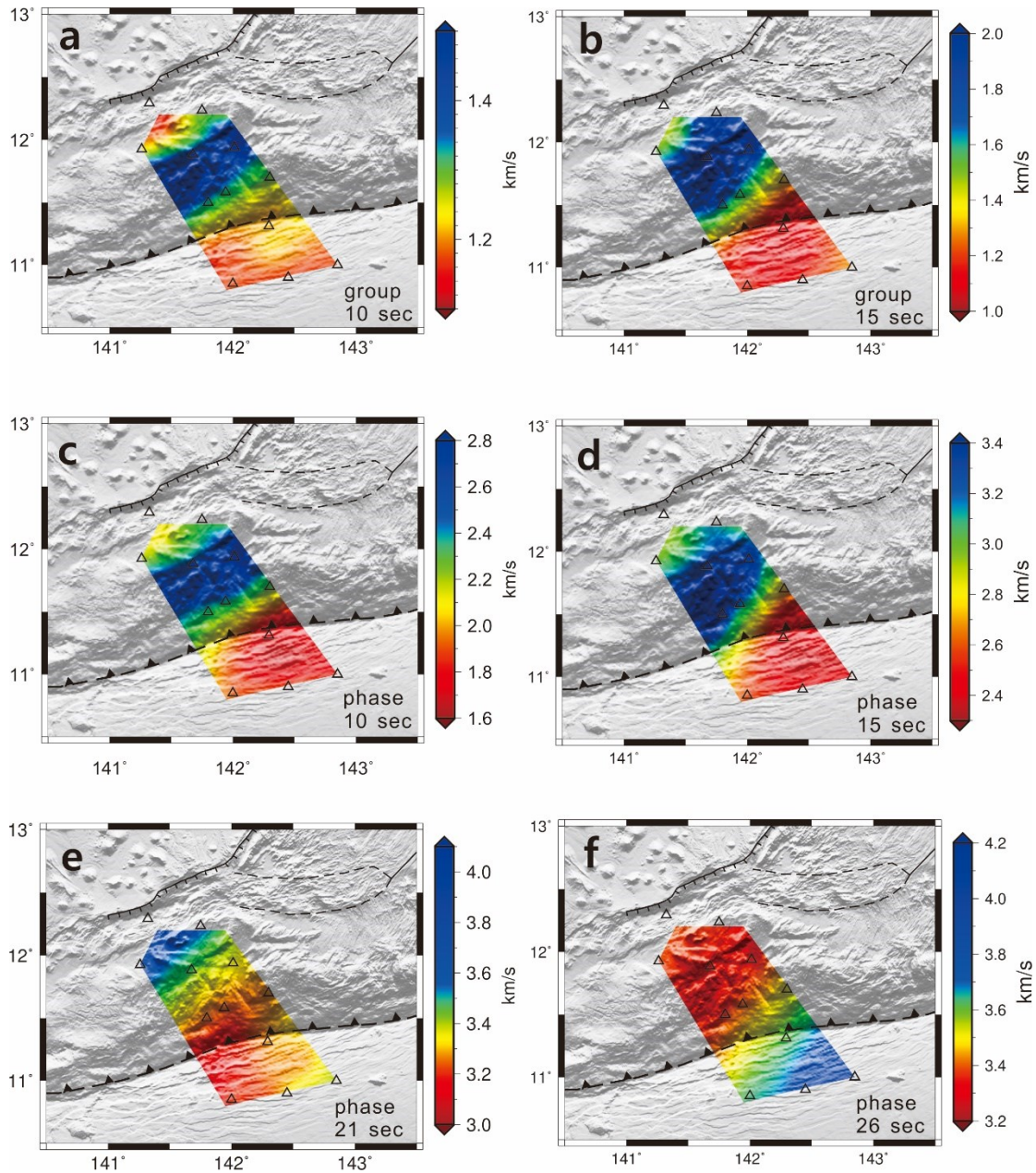


Fig. S3 Maps of the azimuthally averaged group (**a, b**) and phase (**c, d**) velocities at periods of 10 and 15 s inverted by ambient noise tomography. (**e, f**) Maps of azimuthally averaged phase velocities at periods of 21 and 26 s inverted by Eikonal tomography.

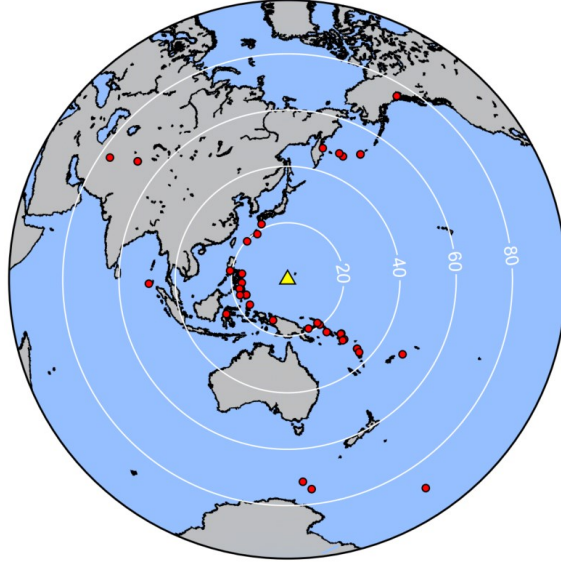


Fig. S4 Earthquakes (red dots) used in this study. The yellow triangle shows the location of the OBS array in southern Mariana.

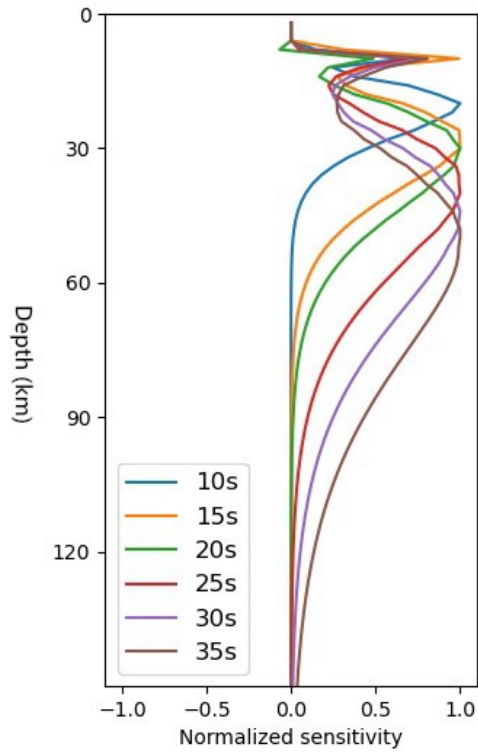


Fig. S5 Phase-velocity sensitivity kernels at example periods, calculated using the average velocity model in Fig. 2b.

Simulation tests for the robustness of a low-velocity zone

We construct two models with the low-velocity zone in the upper mantle, and then run simulations to test whether we could get the low-velocity feature with the same parameterizations in this study. First, we set up two one-dimensional shear-velocity models with a low-velocity mantle layer, one with a linearly increased boundary (Model 1, the solid black lines in Fig. S6 b&d), and one with sharp boundary (Model 2, the solid black lines in Fig. S6 f&h). We calculate the synthetic phase and group dispersion curves, and then apply the Bayesian Monte Carlo inversion with the same parameterizations as in our study to the synthetic phase and group data and obtain a one-dimensional reconstructed shear-velocity structure. The parameterization during Bayesian Monte Carlo inversion is identical to that described in Method. Considering the lacking of observations between periods of 18-21 s, we also conduct the inversion with a gap in dispersion curves to test its effect on inversion (Fig. S6 c&d and g&h). The simulation tests for Model 1 with a linearly increased boundary give an monotonically increasing velocity with depth (Fig. S6 b&d), while the tests for Model 2 with sharp boundary show obviously velocity reduction with depth (Fig. S6 f&h).

The simulation tests suggest that (1) the low-velocity layer can be reconstructed with the same period range of dispersion curves and the same parameterizations in this study, but lack precise depth and thickness resolution; (2) The gap in dispersion curves between periods of 18-21 s has slight influences on the inversion model; (3) The application of the Bayesian Monte Carlo algorithm helps to avoid the potential bias of the starting models. However, it uses a B-spline method to parameterize the upper-mantle V_{sv} , and so may smooth a thin low-velocity layer over a wider depth range; (4) Our observed V_{sv} model is more like Model 1 with a gradually increased low-velocity “boundary”. The gradually increased velocity may be related to decreased serpentinization with depth or possibly because the inversion smoothes a low-velocity layer over a wider depth range.

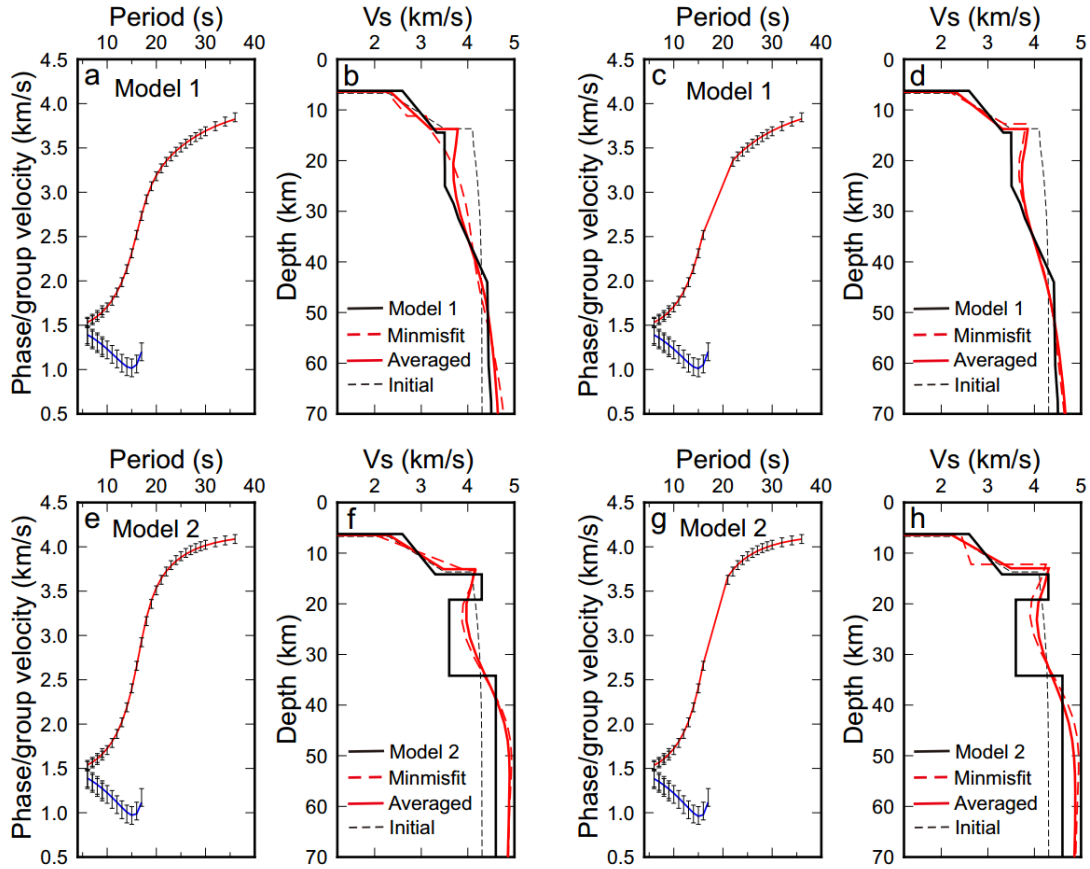


Fig. S6. Robustness test of the low-velocity zone. **(a)** The black error bars are the synthetic phase and group velocities based on the constructed velocity model (solid black line in b). Red and blue lines represent calculated phase and group dispersion curves from Bayesian Monte Carlo inversion with the same parameterizations as in our study based on the one-dimensional reconstructed shear-velocity structure (red solid lines in b). **(b)** The black solid line is the constructed velocity model. The red dashed and solid lines represent the best-fitting and average models from the Monte Carlo inversion of the synthetic dispersion curves, respectively. The black dashed line is the initial model for Monte Carlo inversion. Notions in (c), (e), and (g) are the same as in (a); notions in (d), (f), and (h) are the same as in (b).